

Dynamic Control Allocation Using Constrained Quadratic Programming

Ola Härkegård*

Linköping University, 581 83 Linköping, Sweden

Abstract

Control allocation deals with the problem of distributing a given control demand among an available set of actuators. Most existing methods are static in the sense that the resulting control distribution depends only on the current control demand. In this paper we propose a method for dynamic control allocation, in which the resulting control distribution also depends on the distribution in the previous sampling instant. The method extends regular quadratic programming control allocation by also penalizing the actuator rates. This leads to a frequency dependent control distribution which can be designed to, e.g., account for different actuator bandwidths. The control allocation problem is posed as a constrained quadratic program which provides automatic redistribution of the control effort when one actuator saturates in position or in rate. When no saturations occur, the resulting control distribution coincides with the control demand fed through a linear filter.

*Research engineer, Div. of Automatic Control, Dept. of Electrical Engineering, Linköping University, 581 83 Linköping, Sweden, ola@isy.liu.se, <http://www.control.isy.liu.se/~ola>

Introduction

In recent years, nonlinear flight control design methods, like dynamic inversion¹⁻³ and backstepping,^{4,5} have gained increased attention. These methods result in control laws specifying the moments to be produced in pitch, roll, and yaw, rather than which particular control surface deflections to produce. How to transform these virtual, or generalized, control commands into actual control commands is known as the control allocation problem. Figure 1 illustrates the resulting control configuration.

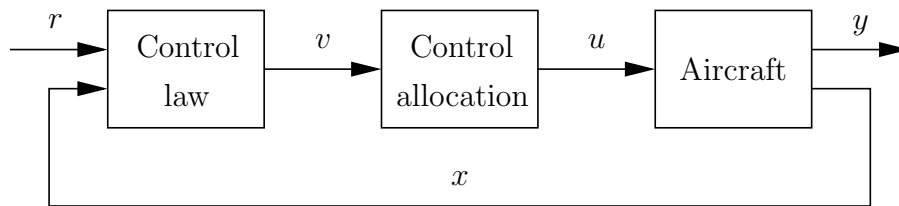


Figure 1. Control configuration when control allocation is used.

With a redundant actuator suite there are several combinations of actuator positions which all produce the same virtual control, and hence give the same overall system behavior. This design freedom is often used to optimize some static performance index, like minimum control, or to prioritize among the actuators. This can be thought of as affecting the distribution of control effect in magnitude among the actuators. Regardless of method (optimization based allocation,⁶⁻¹⁰ daisy chain allocation,¹¹⁻¹³ direct allocation,^{10,14,15} etc.), the resulting mapping from the virtual control command, $v(t)$, to true control input, $u(t)$, can be written as a static relationship

$$u(t) = h(v(t)) \quad (1)$$

A possibility that has been little explored is to also affect the distribution of the control effect in the frequency domain, and use the redundancy to have different actuators operate in

different parts of the frequency spectrum. This requires the mapping from v to u to depend also on previous values of u and v , hence

$$u(t) = h(v(t), u(t - T), v(t - T), u(t - 2T), v(t - 2T), \dots) \quad (2)$$

where T is the sampling interval. We will refer to this as *dynamic control allocation*.

The term dynamic allocation was introduced in Ref. 16, which considers control of marine vessels, equipped with azimuth (rotatable) thrusters. Essentially, the authors use the low frequency component of the total thrust demand to decide the azimuth angles, which are then used to compute the force to be produced by each thruster.

Some flight control examples where filtering has been introduced in the control allocation can also be found in the literature. Ref. 17 considers a case where canards and tailerons are available for pitch control. To achieve a fast initial aircraft response, and to make use of the fast dynamics of the canards, the high frequency component of the required pitching moment is fed to the canards while the remaining low frequency component is fed to the tailerons, which are used solely at trimmed flight.

Another example can be found in Ref. 18, where thrust vectored control (TVC) is available. To prevent the TVC vanes from suffering thermal damage from the jet exhaust, the TVC deflection command is fed to a wash-out filter (static gain zero), so that the vanes do not remain deflected on the exhaust for long periods of time.

In Ref. 19, rate saturation problems are used as a motivation for dynamic control allocation, or frequency-apportioned control allocation, as the authors call it. The high and low frequency components of the moment demand are each multiplied by a weighted pseudoinverse of the control effectiveness matrix, B , with the weights based on the rate and position bounds of the actuators, respectively. With this strategy, fast actuators are used for high frequency control, and the chances of rate saturation are reduced.

Hence, there are practical cases where dynamic control allocation is desirable. In this paper, a new systematic method for dynamic control allocation is proposed. The method is an extension of regular quadratic programming control allocation. The key idea is to add an extra term to the optimization criterion to also penalize actuator rates. When no saturations occur, the control allocation mapping becomes a linear filter of the form

$$u(t) = Fu(t - T) + Gv(t) \quad (3)$$

from the virtual control command v to the actuator commands u . The frequency characteristics of this filter are decided by weighting matrices selected by the control designer. Thus, unlike most previous methods, no filters are to be explicitly constructed by the control designer.

Two design examples are included to illustrate the potential benefits of using the proposed scheme for dynamic control allocation.

Control Allocation Problem Formulation

As stated in the introduction, an important application of control allocation is nonlinear flight control. Consider a general nonlinear dynamical model of an aircraft given by

$$\dot{x} = f(x, \delta) \quad (4a)$$

$$\dot{\delta} = g(\delta, u) \quad (4b)$$

where x = aircraft state vector, δ = actuator positions, and u = commanded actuator positions. To incorporate the actuator position and rate constraints we impose that

$$\delta_{\min} \leq \delta \leq \delta_{\max}, \quad |\dot{\delta}| \leq \delta_{\text{rate}} \quad (5)$$

where δ_{\min} and δ_{\max} are the lower and upper position constraints, and δ_{rate} specifies the maximal individual actuator rates.

Even in the case when f and g are linear, it is nontrivial to design a control law which gives the desired closed loop dynamics while assuring that the actuator constraints are met. A common approach is therefore to split the design task into two subtasks. Neglecting the typically fast actuator dynamics, i.e., assuming $\delta = u$, and viewing the actuators as pure moment generators yields the approximate model

$$\dot{x} = f_M(x, M(x, u)) \quad (6)$$

where $M(x, u)$ is the mapping from the commanded actuator positions to the resulting aerodynamic moment acting on the aircraft and f_M describes how the aerodynamic moment affects the aircraft dynamics.

The control design can now be performed in two steps. First, design a control law in terms of the moment to be produced,

$$M(x, u) = k(r, x) \quad (7)$$

that yields some desired closed loop dynamics, where $r = \text{pilot command}$. Second, determine u , constrained by (5) (with $\delta = u$), that satisfies (7).

The latter step is the control allocation step. Since modern aircraft use digital control systems, it is reasonable to merge the constraints (5) into an overall time varying position constraint given by

$$\underline{u}(t) \leq u(t) \leq \bar{u}(t) \quad (8)$$

where

$$\underline{u}(t) = \max\{\delta_{\min}, u(t - T) - \delta_{\text{rate}}T\} \quad (9a)$$

$$\bar{u}(t) = \min\{\delta_{\max}, u(t - T) + \delta_{\text{rate}}T\} \quad (9b)$$

and T is the sampling time.¹² To simplify the search for a feasible solution to (7) we assume the aerodynamic moment to be affine in the controls. With this, the equation to be solved for u becomes

$$M(x, u) = B(x)u + c(x) = k(r, x) \quad (10)$$

or, equivalently,

$$Bu(t) = v(t) \quad (11)$$

where $v(t) = k(r, x) - c(x)$ is the virtual control command computed from the control law (7).

Now, to perform on-line control allocation we wish to determine, at each sampling instant, a control command $u(t)$ which is feasible with respect to the actuator constraints (8) and that satisfies (11), if possible.

Dynamic Control Allocation

The dynamic control allocation method that we propose can be posed as a sequential quadratic programming problem:

$$u(t) = \arg \min_{u(t) \in \Omega} \left(\|W_1(u(t) - u_s(t))\|^2 + \|W_2(u(t) - u(t - T))\|^2 \right) \quad (12a)$$

$$\Omega = \arg \min_{\underline{u}(t) \leq u(t) \leq \bar{u}(t)} \|W_v(Bu(t) - v(t))\| \quad (12b)$$

where $u \in \mathbb{R}^m$ is the true control input, $u_s \in \mathbb{R}^m$ is the desired steady state control input, $v \in \mathbb{R}^k$ is the virtual control command, $B \in \mathbb{R}^{k \times m}$ is the control effectiveness matrix, and W_1 , W_2 , and W_v are square matrices of the proper dimensions. B is assumed to have full row rank k . $\|\cdot\|$ denotes the Euclidean 2-norm defined by $\|u\| = \sqrt{u^T u}$.

Equation (12) should be interpreted as follows: Given Ω , the set of feasible control inputs (with respect to position and rate constraints) that minimize the virtual control error $Bu(t) - v(t)$ (weighted by W_v), pick the control input that minimizes the cost function in (12a).

Hence, satisfying the virtual control demand (11) has the highest priority. When this is not possible due to the actuator constraints, (12b) corresponds to solving (11) in the least squares sense. The design matrix W_v can then be used to affect the way that command limiting is performed by weighting the virtual control errors differently to prioritize certain components of v .

When there are several control inputs that give the same virtual control error (not necessarily zero), i.e., when Ω does not contain only a single point, u is made unique by minimizing the criterion in (12a). This criterion is a mix of 1) keeping the control input close to the desired steady state value u_s , and 2) minimizing the change in the control input compared to the previous sampling instant. The trade-off between these two requirements is governed by the weighting matrices W_1 and W_2 . A large diagonal entry in W_1 will make the corresponding actuator converge quickly to its desired position while a large W_2 entry will prevent the actuator from moving too quickly. Note however that these weighting matrices only affect the control input if u is not uniquely determined by (12b). The following assumption certifies that the overall control allocation problem (12) has a unique optimal solution.

Assumption 1 *Assume that the weighting matrices W_1 and W_2 are symmetric and such*

that

$$W = (W_1^2 + W_2^2)^{1/2} \quad (13)$$

is nonsingular.

The symmetry assumption is no restriction since if, e.g., W_1 is not symmetric, it can be replaced by the symmetric matrix square root $(W_1^T W_1)^{1/2}$ without affecting the solution.

Equation (12) specifies which solution to the control allocation problem that is sought but not how to find it. To actually solve the optimization problem, the two terms in (12a) can first be merged into one term without affecting the solution. Then, any QP solver suitable for real-time implementation^{6,7,9,20} can be used to find the solution. Since the optimization problem (12) is to be solved at each sampling instant, no variables need to be constant. This means that the control efficiency matrix B can be updated continuously, which allows for reconfiguration after an actuator failure, and that different weighting matrices can be used for different flight cases.

By including the previous control input in the optimization problem (12), the resulting control distribution will clearly be a mapping of the form

$$u(t) = h(v(t), u(t - T)) \quad (14)$$

It is important to point out that despite the control allocator now being a dynamical system, no extra lag is introduced into the control loop since minimizing the virtual control error has top priority in (12).

Let us now investigate some characteristics of the discrete time dynamical system (14). In the following section we consider the nonsaturated case in which h can be found analytically, and investigate the issues of stability and steady state distribution.

The Nonsaturated Case

If no actuators are saturated in the solution to (12), the actuator constraints can be disregarded and the optimization problem reduces to

$$\min_{u(t)} \left(\|W_1(u(t) - u_s(t))\|^2 + \|W_2(u(t) - u(t - T))\|^2 \right) \quad (15a)$$

$$\text{subject to } Bu(t) = v(t) \quad (15b)$$

Explicit Solution

Having removed the actuator constraints, one can derive a closed form solution to (15).

Theorem 1 *Let Assumption 1 hold. Then the control allocation problem (15) has the solution*

$$u(t) = Eu_s(t) + Fu(t - T) + Gv(t) \quad (16)$$

where

$$E = (I - GB)W^{-2}W_1^2 \quad (17)$$

$$F = (I - GB)W^{-2}W_2^2 \quad (18)$$

$$G = W^{-1}(BW^{-1})^\dagger \quad (19)$$

Proof: It is straightforward to show that the cost function in (15a) has the same minimizer as $\|W(u(t) - u_0(t))\|$ where

$$W = (W_1^2 + W_2^2)^{1/2}$$

$$u_0(t) = W^{-2}(W_1^2 u_s(t) + W_2^2 u(t - T))$$

Now, adding the linear constraint (15b), where B has full row rank, gives the weighted, shifted pseudoinverse solution

$$u(t) = (I - GB)u_0(t) + Gv(t)$$

$$G = W^{-1}(BW^{-1})^\dagger$$

from which it follows that

$$u(t) = \underbrace{(I - GB)W^{-2}W_1^2}_{E} u_s(t) + \underbrace{(I - GB)W^{-2}W_2^2}_{F} u(t - T) + Gv(t)$$

which completes the proof. A more detailed proof can be found in Ref. 21. ■

The \dagger symbol denotes the pseudoinverse operator defined as²² $B^\dagger = B^T(BB^T)^{-1}$ for a $k \times m$ matrix B with full row rank k .

The theorem shows that the optimal solution to the control allocation problem (15) is given by the linear filter (16). The properties of this filter will be investigated in the two following sections.

Dynamic Properties

Let us first study the dynamic properties of the filter (16). Note that the optimization criterion in (15) does not consider future values of $u(t)$. It is therefore not obvious that the resulting filter (16) is stable. The poles of the filter, which can be found as the eigenvalues of the matrix F , are characterized by the following theorem.

Theorem 2 *Let F be defined as in Theorem 1 and let Assumption 1 hold. Then the eigenvalues of F , $\lambda(F)$, satisfy*

$$0 \leq \lambda(F) \leq 1 \tag{20}$$

If W_1 is nonsingular, the upper eigenvalue limit becomes strict, i.e.,

$$0 \leq \lambda(F) < 1 \quad (21)$$

Proof: We wish to characterize the eigenvalues of

$$\begin{aligned} F &= (I - GB)W^{-2}W_2^2 \\ &= (I - W^{-1}(BW^{-1})^\dagger B)W^{-2}W_2^2 \\ &= W^{-1}(I - (BW^{-1})^\dagger BW^{-1})W^{-1}W_2^2 \end{aligned} \quad (22)$$

Let the singular value decomposition of BW^{-1} be given by

$$BW^{-1} = U\Sigma V^T = U \begin{bmatrix} \Sigma_r & 0 \end{bmatrix} \begin{bmatrix} V_r^T \\ V_0^T \end{bmatrix} = U\Sigma_r V_r^T$$

where U and V are orthogonal matrices and Σ_r is a $k \times k$ diagonal matrix with strictly positive diagonal entries (since BW^{-1} has rank k). This yields

$$I - (BW^{-1})^\dagger BW^{-1} = I - V_r \Sigma_r^{-1} U^T U \Sigma_r V_r^T = I - V_r V_r^T = V_0 V_0^T$$

since $VV^T = V_r V_r^T + V_0 V_0^T = I$. Inserting this into (22) gives us

$$F = W^{-1} V_0 V_0^T W^{-1} W_2^2$$

Now use the fact²³ that the nonzero eigenvalues of a matrix product AB , $\lambda_{nz}(AB)$, satisfy $\lambda_{nz}(AB) = \lambda_{nz}(BA)$ to get

$$\lambda_{nz}(F) = \lambda_{nz}(V_0^T W^{-1} W_2^2 W^{-1} V_0)$$

From the definition of singular values we get

$$\lambda(V_0^T W^{-1} W_2^2 W^{-1} V_0) = \sigma^2(W_2 W^{-1} V_0) \geq 0$$

This shows that the nonzero eigenvalues of F are real and positive and thus, $\lambda(F) \geq 0$ holds.

What remains to show is that the eigenvalues of F are bounded by 1. To do this we investigate the maximum eigenvalue, $\bar{\lambda}(F)$.

$$\bar{\lambda}(F) = \bar{\sigma}^2(W_2 W^{-1} V_0) = \|W_2 W^{-1} V_0\|^2 \leq \|W_2 W^{-1}\|^2 \|V_0\|^2$$

Since

$$\|V_0\|^2 = \underbrace{\bar{\lambda}(V_0^T V_0)}_I = 1$$

we get

$$\bar{\lambda}(F) \leq \|W_2 W^{-1}\|^2 = \sup_{x \neq 0} \frac{x^T W^{-1} W_2^2 W^{-1} x}{x^T x}$$

Introducing $y = W^{-1} x$ yields

$$\bar{\lambda}(F) \leq \sup_{y \neq 0} \frac{y^T W_2^2 y}{y^T W^2 y} = \sup_{y \neq 0} \frac{y^T W_2^2 y}{y^T W_1^2 y + y^T W_2^2 y} \leq \sup_{y \neq 0} \frac{y^T W_2^2 y}{y^T W_2^2 y} = 1$$

since $y^T W_1^2 y = \|W_1 y\|^2 \geq 0$ for any symmetric W_1 . If W_1 is nonsingular, we get $y^T W_1^2 y = \|W_1 y\|^2 > 0$ for $y \neq 0$ and the last inequality becomes strict, i.e., $\bar{\lambda}(F) < 1$ in this case. ■

The theorem states that the poles of the linear control allocation filter (16) lie between 0 and 1 on the real axis. This has two important practical implications:

- If W_1 is nonsingular the filter poles lie strictly inside the unit circle. This implies that the filter is asymptotically stable, which means that the actuator responses will be bounded for a bounded virtual control command. If W_1 is singular, only neutral

stability can be guaranteed (although asymptotic stability may hold).

- The fact that the poles lie on the positive real axis implies that the actuator responses to a step in the virtual control input are not oscillatory.

Steady State Properties

In the previous section we showed that the control allocation filter (16) is asymptotically stable under mild assumptions. Let us therefore investigate the steady state solution for a constant virtual control input.

Theorem 3 *Let u_s satisfy*

$$Bu_s = v_0 \tag{23}$$

where $v(t) = v_0$ is the desired virtual control input. Then, if W_1 is nonsingular, the steady state control distribution of (16) is given by

$$\lim_{t \rightarrow \infty} u(t) = u_s \tag{24}$$

Proof: If W_1 is nonsingular, the linear filter (16) is asymptotically stable according to Theorem 2. This means that in the limit, $u(t) = u(t - T)$ holds. Then (15) reduces to

$$\begin{aligned} \min_u \quad & \|W_1(u - u_s)\|^2 \\ \text{subject to} \quad & Bu = v_0 \end{aligned} \tag{25}$$

If u_s satisfies $Bu_s = v_0$, then $u = u_s$ is obviously one optimal solution to (25). Further, if W_1 is nonsingular, $u = u_s$ is the unique optimal solution. ■

Since u_s can be time varying in (12), the theorem condition (23) can be fulfilled by selecting $u_s(t) = Sv(t)$ where $BS = I$. For example, selecting $S = B^\dagger$ minimizes the

control input norm $\|u\|$ at steady state. If u_s does not satisfy (23), the steady state control distribution will also depend on W_1 . This is undesirable since it makes the role of the design parameter W_1 unclear.

Design Examples

Let us now apply the proposed method to two different design examples to see what dynamic control allocation can offer and how to select the tuning variables.

Actuator Dynamics

One application of dynamic control allocation is to account for actuator dynamics. Actuator dynamics can be an obstacle to performing control allocation since most allocation schemes – including the one proposed in this paper – assume a static relationship between the actuator commands and the resulting total control effort, see (11). Disregarding these dynamics in cases when one or several of the actuators has a low bandwidth may deteriorate the overall system behavior, and possibly even lead to instability.

A previously proposed strategy is to modify the natural actuator dynamics, using feedback or feedforward compensation, or a combination of the two, to effectively increase the actuator bandwidth. This has proven to work well in several applications.^{24–26} However, there are situations when this is not practically feasible solution. In this section we consider one such example and show that combining this type of compensation with dynamic control allocation can give better results.

Consider the system depicted in Figure 2, with two actuators whose outputs, u_1^a and u_2^a , produce a total control effort of

$$v^a = 2u_1^a + u_2^a = Bu^a, \quad B = \begin{bmatrix} 2 & 1 \end{bmatrix} \quad (26)$$

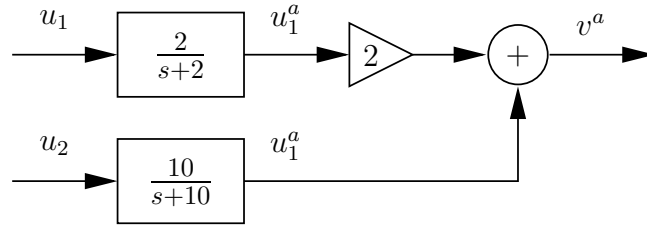


Figure 2. System with one slow and one fast actuator.

The actuators have first order dynamics and their bandwidths are 2 rad/s and 10 rad/s, respectively. Thus, the first actuator is slow but effective while the second one is fast but less effective. The actuator position limits are given by $|u_1^a| \leq 1$, $|u_2^a| \leq 2$.

Assume now that the dynamics of the second actuator are fast enough to be disregarded for the application in mind, but not the dynamics of the first actuator. As discussed above, this can be resolved by precompensating the first actuator command with the inverse of the present dynamics (time discretized) times the desired actuator transfer function, which we select to be the same as for the fast actuator. Figure 3 shows the overall system structure. Now that both actuators have a bandwidth of 10 rad/s, the same is true for the total transfer function from v to v^a .

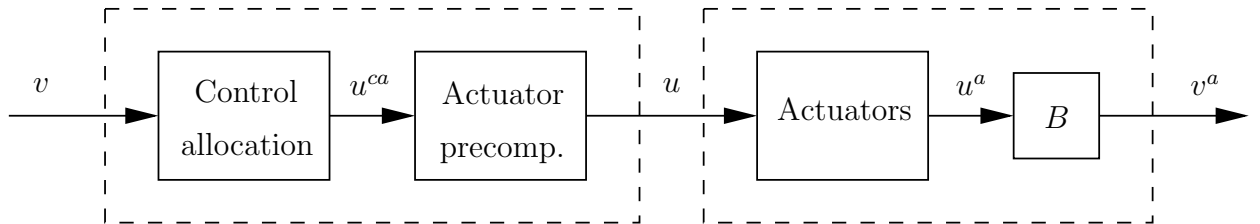


Figure 3. Overall system configuration.

Figure 4 (top) shows the response to a smoothed step in the virtual control command, v , when a static control allocator is used ($u_s = 0$, $W_1 = I$, $W_2 = 0$, and $W_v = 1$ in (12)) and

the sampling time is $T = 0.02$ s. Both actuator outputs satisfy the position constraints and the produced control effort v^a (bottom) responds as expected to the command. However, in a practical situation there may be additional constraints which makes this an undesirable solution. For example, if the actuators are electrical motors, the large position error in the first actuator response may lead to an input voltage that is infeasible.

To account for the difference in bandwidth in a more suitable way, let us design a dynamic control allocator which uses both actuators to produce the low frequency part of the total control demand, but only the fast actuator for the high frequency part. This can be accomplished by selecting the tuning parameters in (12) as

$$u_s(t) = B^\dagger v(t), \quad W_1 = \text{diag}(1, 1), \quad W_2 = \text{diag}(12, 0), \quad W_v = 1 \quad (27)$$

The precompensation of the first actuator command is still necessary in order to smoothly merge the two actuator responses. The overall discrete time transfer functions from the virtual control command v to the actuator commands u are shown in Figure 5. Figure 4 (middle) shows the resulting step response. Initially, the fast actuator is used to produce most of the control effort, but after about 3 s the actuator commands have converged to the desired static distribution which is the same as before, $u(t) = B^\dagger v(t)$. Thus, without affecting the static control distribution between the actuators, the transient distribution has been designed to better account for the difference in actuator bandwidth.

Figure 6 shows the response when $v = 3$ is commanded. This choice makes the desired steady state distribution u_s infeasible. As seen from the figure, the algorithm responds by utilizing the second actuator more to compensate for the saturated first actuator.

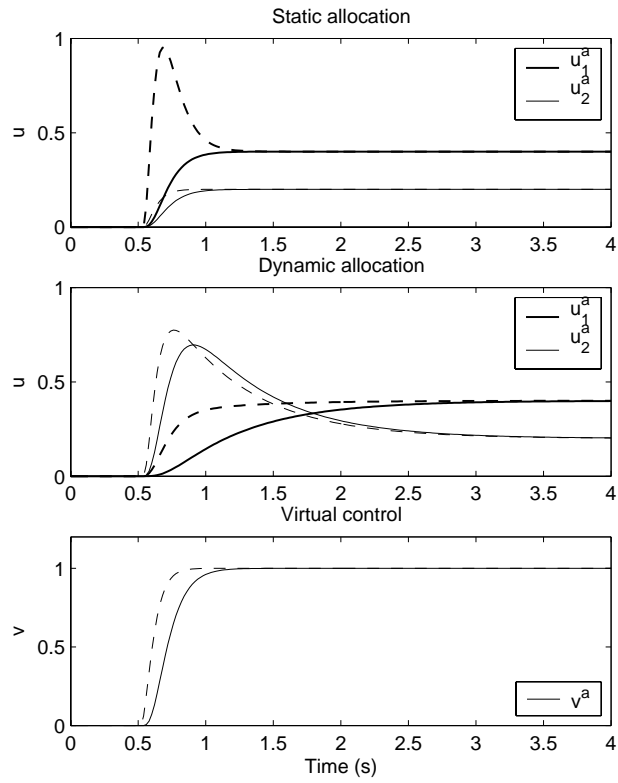


Figure 4. Simulation results for static and dynamic allocation. Dashed: commanded values. Solid: actual values.

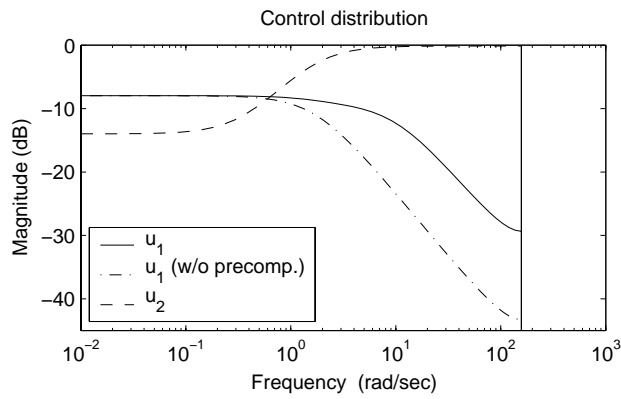


Figure 5. Transfer functions from v to u with dynamic allocation.

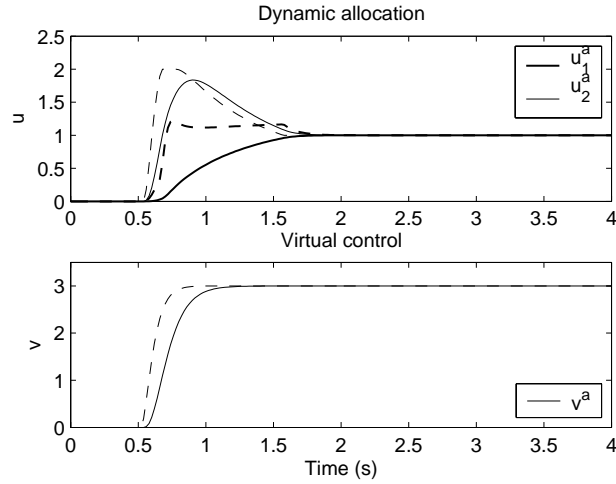


Figure 6. Control allocation results for $v = 3$. Dashed: commanded values. Solid: actual values.

Multivariable Flight Control

Let us now consider a flight control example. The purpose of the example is to show that it is straightforward to apply dynamic control allocation also in a multivariable case, and to illustrate the benefits of using control allocation in general.

The ADMIRE model,²⁷ developed by the Swedish Defence Research Agency (FOI), is used for simulation. ADMIRE is a MATLAB/Simulink based model of a small single engine fighter aircraft with a delta canard configuration, and includes actuator dynamics and nonlinear aerodynamics. The existing baseline control system is used to compute the aerodynamic moment coefficients, $M(x, u_{\text{Adm}})$, to be produced in roll, pitch, and yaw, see Figure 7. Since the baseline control system does not take actuator constraints into account, u_{Adm} may be infeasible. Given M , the control allocator solves (12) for the commanded control surface deflections, u .

The model parameters B and c in (10) are recomputed at each sampling instant by linearizing $M(x, u)$ around the current state vector and the current control surface position

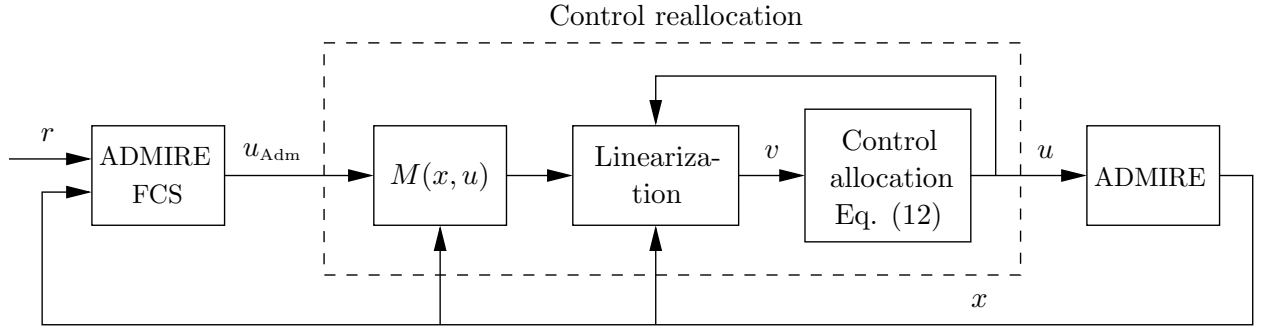


Figure 7. Overview of the closed loop system used for simulation.

vector. In the ADMIRE model the sampling time is $T = 0.02$ s. The constrained least squares problem (12) is solved at each sampling instant using the weighted least squares active set solver from Ref. 20.

The control input consists of the commanded deflections for the canard wings (u_1), the right elevons (u_2), the left elevons (u_3), and for the rudder (u_4). The actuator position and rate constraints in (5) are given by

$$\delta_{\min} = \begin{pmatrix} -55 & -30 & -30 & -30 \end{pmatrix}^T \cdot \frac{\pi}{180} \text{ rad} \quad (28)$$

$$\delta_{\max} = \begin{pmatrix} 25 & 30 & 30 & 30 \end{pmatrix}^T \cdot \frac{\pi}{180} \text{ rad} \quad (29)$$

$$\delta_{\text{rate}} = \begin{pmatrix} 50 & 150 & 150 & 100 \end{pmatrix}^T \cdot \frac{\pi}{180} \text{ rad/s} \quad (30)$$

At trimmed flight at Mach 0.4, 1000 m, the control effectiveness matrix, containing the partial derivatives of the aerodynamic moment coefficients in roll (C_l), pitch (C_m), and yaw

(C_n) with respect to the control inputs, is given by

$$B = 10^{-2} \times \begin{pmatrix} 0 & -9.0 & 9.0 & 2.7 \\ 19.7 & -22.4 & -22.4 & 0 \\ 0 & -3.3 & 3.3 & -8.0 \end{pmatrix} \text{rad}^{-1} \quad (31)$$

from which it can be seen, for example, that the elevons are the most effective actuators for producing rolling moment while the rudder provides good yaw control, as expected. This is the B -matrix used in the design and analysis of the control allocation filter below.

Let us now consider the requirements regarding the control distribution. At trimmed flight, it is beneficial not to deflect the canards at all to achieve low drag. We therefore select the steady state distribution u_s as the solution to

$$\begin{aligned} \min_{u_s} \quad & \|u_s\| \\ \text{subject to} \quad & Bu_s = v \\ & u_{s,1} = 0 \end{aligned} \quad (32)$$

which yields

$$u_s(t) = Sv(t), \quad S = \begin{pmatrix} 0 & 0 & 0 \\ -5.0 & -2.2 & -1.7 \\ 5.0 & -2.2 & 1.7 \\ 4.1 & 0 & -11.2 \end{pmatrix} \quad (33)$$

During maneuvering, corresponding to higher frequencies of v , we seek a distribution that splits the pitch command between the canards and the elevons. Further, since the elevons have a higher rate limit than the rudder we put a higher rate penalty on the rudder.

Selecting

$$W_1 = \text{diag}(2, 2, 2, 2) \quad (34)$$

$$W_2 = \text{diag}(8, 10, 10, 20) \quad (35)$$

and using Theorem 1 yields the control allocation filter

$$u(t) = Fu(t - T) + G_{\text{tot}}v(t) \quad (36)$$

where

$$F = 10^{-1} \times \begin{pmatrix} 5.9 & 4.1 & 4.1 & 0 \\ 2.6 & 1.8 & 1.8 & 0 \\ 2.6 & 1.8 & 1.8 & 0 \\ 0 & 0 & 0 & 0 \end{pmatrix} \quad (37)$$

$$G_{\text{tot}} = G + ES = \begin{pmatrix} 0 & 1.8 & 0 \\ -5.0 & -1.4 & -1.7 \\ 5.0 & -1.4 & 1.7 \\ 4.1 & 0 & -11.2 \end{pmatrix} \quad (38)$$

in the nonsaturated case. The eigenvalues of F are given by

$$\lambda(F) = 0, 0, 0, 0.95 \quad (39)$$

which is in agreement with Theorem 2. Note that the number of nonzero eigenvalues (one) is equal to the dimension of the nullspace of B .

The frequency characteristics of the filter are illustrated in Figure 8, which shows a

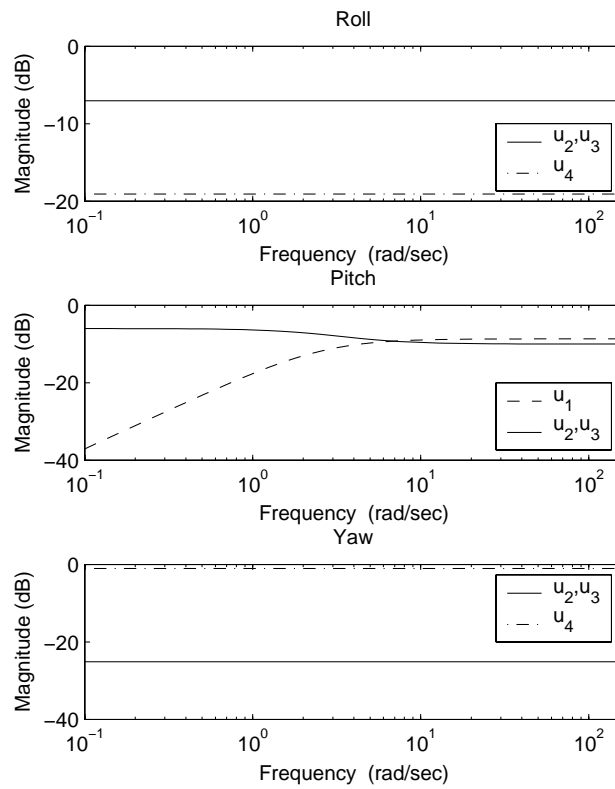


Figure 8. Dynamic control allocation transfer functions from v (moment coefficients) to u (control surface commands).

magnitude plot of the transfer functions from v to u . Each transfer function has been weighted with its corresponding entry in B to show the proportion of v that the actuator produces. As desired, the steady state gain is zero for the canards while at frequencies above 5 rad/s the pitch command is evenly distributed between the canards and the left and right elevons. In roll and yaw, the control distribution does not depend on the frequency despite that the rate penalty for the rudder was selected higher than for the elevons. This is due to that effectively only two control options – rudder and differential elevons – are available for lateral control. These controls are therefore determined completely by the commands in roll and yaw and are not affected by the choice of W_1 and W_2 .

The final tuning variable, W_v , which does not affect the solution in the nonsaturated case, is selected as

$$W_v = \text{diag}(1, 10, 1) \quad (40)$$

This puts the highest priority on producing the pitch command correctly.

Figure 9 shows the simulation results from a full pitch up command followed by a full roll command. When dynamic control allocation is used, the initial response of the canards and the elevons to the pitch command are of about the same size, while at steady state the canards are not used at all, in accordance with the designed frequency distributions.

Let us now compare the results from using dynamic control allocation with those obtained by the baseline control system without reallocation, also shown in Figure 9. The response to the pitch command at $t = 1$ s is virtually the same in both cases. Although the control surface position plots differ slightly, the same aerodynamic moment is produced in both cases. When the roll command is applied at $t = 3$ s, the left elevons saturate in both cases. Whereas the baseline control system does not take this into account, the control allocator responds by redistributing the control effect to the remaining three actuators. This gives a faster reduction of the pitch rate and a smaller undershoot. In fact, investigations show that

with control allocation the virtual control demand (11) is satisfied at all times except just after 3s and 5s where the roll and yaw commands cannot be produced exactly.

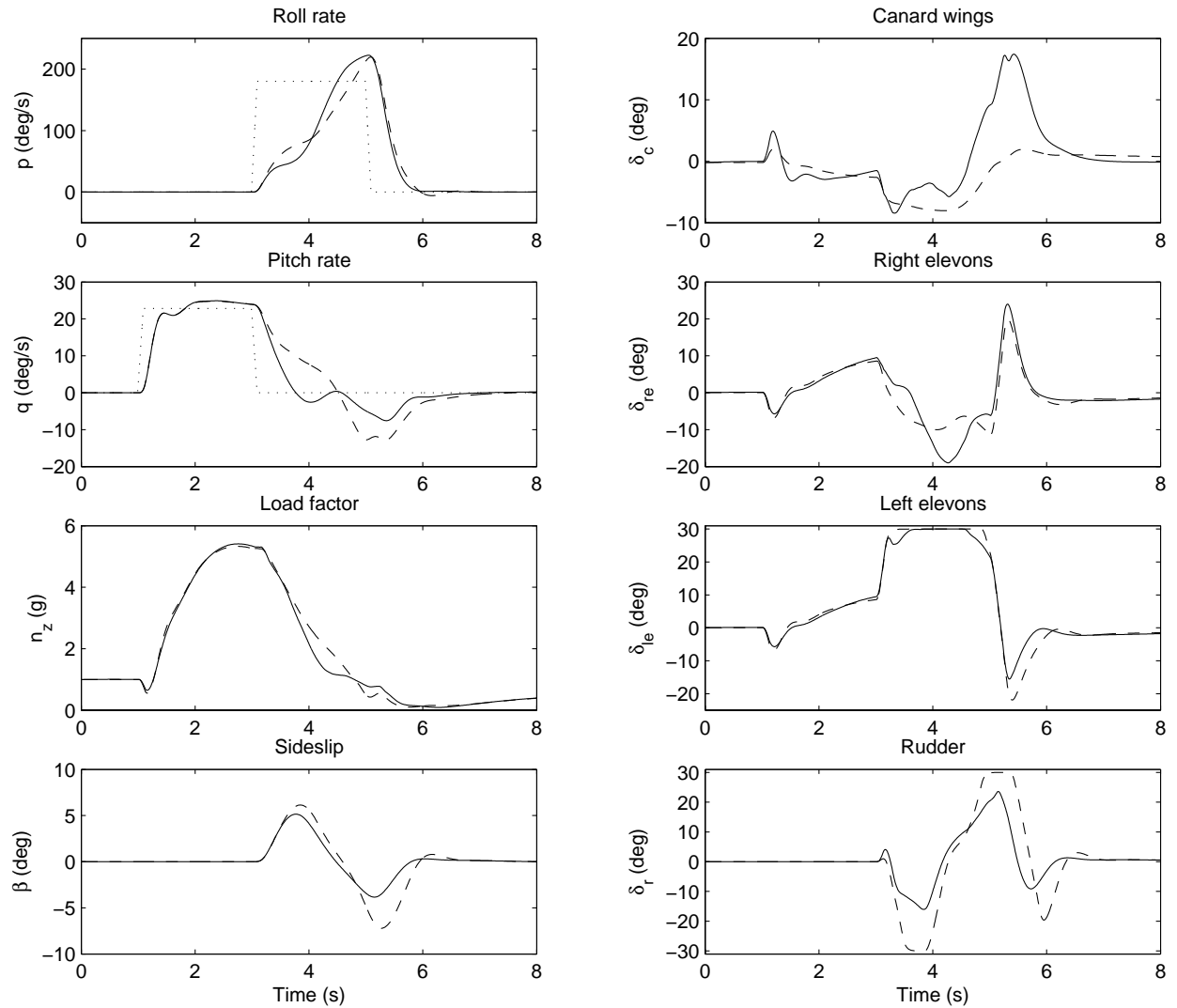


Figure 9. Simulation results for dynamic control allocation (solid) and for the baseline control system (dashed).

Conclusions

In this paper a new method for dynamic control allocation has been presented. Dynamic control allocation offers an extra degree of freedom compared to static control allocation in that the distribution of control effort among the actuators need not be the same for all frequencies. One area of use is compensating for actuator dynamics, as illustrated in one of the design examples.

When no actuators saturate, the control allocator becomes a stable linear filter whose frequency characteristics are decided by tuning variables selected by the user. The problem formulation guarantees that the different transfer functions are complementary which makes it easy to apply the method also in a multivariable case.

Further, since the allocation problem is posed as a quadratic program, it is straightforward to consider actuator position and rate constraints in order to achieve redistribution of the control effort when one actuator saturates, and to perform command limiting when the control demand cannot be satisfied.

References

- ¹Meyer, G., Su, R., and Hunt, L. R., "Application of nonlinear transformations to automatic flight control," *Automatica*, Vol. 20, No. 1, 1984, pp. 103–107.
- ²Lane, S. H. and Stengel, R. F., "Flight control design using non-linear inverse dynamics," *Automatica*, Vol. 24, No. 4, 1988, pp. 471–483.
- ³Enns, D., Bugajski, D., Hendrick, R., and Stein, G., "Dynamic inversion: an evolving methodology for flight control design," *International Journal of Control*, Vol. 59, No. 1, Jan. 1994, pp. 71–91.
- ⁴Härkegård, O. and Glad, S. T., "A backstepping design for flight path angle control," *Proc. of the 39th Conference on Decision and Control*, Sydney, Australia, Dec. 2000, pp. 3570–3575.
- ⁵Härkegård, O. and Glad, S. T., "Flight control design using backstepping," *Proc. of the IFAC NOL-COS'01*, St. Petersburg, Russia, July 2001.

⁶Virnig, J. C. and Bodden, D. S., “Multivariable control allocation and control law conditioning when control effectors limit,” *AIAA Guidance, Navigation, and Control Conference and Exhibit*, Scottsdale, AZ, Aug. 1994.

⁷Enns, D., “Control allocation approaches,” *AIAA Guidance, Navigation, and Control Conference and Exhibit*, Boston, MA, 1998, pp. 98–108.

⁸Ikeda, Y. and Hood, M., “An application of L1 optimization to control allocation,” *AIAA Guidance, Navigation, and Control Conference and Exhibit*, Denver, CO, Aug. 2000.

⁹Burken, J. J., Lu, P., Wu, Z., and Bahm, C., “Two reconfigurable flight-control design methods: Robust servomechanism and control allocation,” *Journal of Guidance, Control, and Dynamics*, Vol. 24, No. 3, May–June 2001, pp. 482–493.

¹⁰Bodson, M., “Evaluation of optimization methods for control allocation,” *Journal of Guidance, Control, and Dynamics*, Vol. 25, No. 4, July–Aug. 2002, pp. 703–711.

¹¹Adams, R. J., Buffington, J. M., and Banda, S. S., “Design of nonlinear control laws for high-angle-of-attack flight,” *Journal of Guidance, Control, and Dynamics*, Vol. 17, No. 4, 1994, pp. 737–746.

¹²Durham, W. C. and Bordignon, K. A., “Multiple control effector rate limiting,” *Journal of Guidance, Control, and Dynamics*, Vol. 19, No. 1, Jan.–Feb. 1996, pp. 30–37.

¹³Buffington, J. M. and Enns, D. F., “Lyapunov stability analysis of daisy chain control allocation,” *Journal of Guidance, Control, and Dynamics*, Vol. 19, No. 6, Nov.–Dec. 1996, pp. 1226–1230.

¹⁴Durham, W. C., “Constrained control allocation,” *Journal of Guidance, Control, and Dynamics*, Vol. 16, No. 4, July–Aug. 1993, pp. 717–725.

¹⁵Durham, W. C., “Constrained control allocation: Three moment problem,” *Journal of Guidance, Control, and Dynamics*, Vol. 17, No. 2, March–April 1994, pp. 330–336.

¹⁶Berge, S. P. and Fossen, T. I., “Robust control allocation of overactuated ships: Experiments with a model ship,” *Proc. of the 4th IFAC Conference on Manoeuvring and Control of Marine Craft*, Brijuni, Croatia, Sept. 1997.

¹⁷Papageorgiou, G., Glover, K., and Hyde, R. A., “The \mathcal{H}_∞ loop-shaping approach,” *Robust Flight Control: A Design Challenge*, edited by J.-F. Magni, S. Bannani, and J. Terlouw, chap. 29, Springer, 1997, pp. 464–483.

¹⁸Reiner, J., Balas, G. J., and Garrard, W. L., “Flight control design using robust dynamic inversion and time-scale separation,” *Automatica*, Vol. 32, No. 11, 1996, pp. 1493–1504.

¹⁹Davidson, J. B., Lallman, F. J., and Bundick, W. T., “Integrated reconfigurable control allocation,” *AIAA Guidance, Navigation, and Control Conference and Exhibit*, Montreal, Canada, Aug. 2001.

²⁰Härkegård, O., “Efficient active set algorithms for solving constrained least squares problems in aircraft control allocation,” *Proc. of the 41st IEEE Conference on Decision and Control*, Las Vegas, NV, Dec. 2002, pp. 1295–1300.

²¹Härkegård, O., *Backstepping and Control Allocation with Applications to Flight Control*, PhD thesis no. 820, Department of Electrical Engineering, Linköping University, May 2003.

²²Björck, Å., *Numerical Methods for Least Squares Problems*, SIAM, 1996, pp. 15–17.

²³Zhang, F., *Matrix Theory: Basic results and techniques*, Springer, 1999, p. 51.

²⁴Bolling, J. G., *Implementation of Constrained Control Allocation Techniques Using Aerodynamic Model of an F-15 Aircraft*, Master’s thesis, Virginia Polytechnic Institute and State University, 1997.

²⁵Venkataraman, R. and Doman, D. B., “Control allocation and compensation for over-actuated systems with non-linear effectors,” *Proc. of the American Control Conference*, Arlington, VA, June 2001, pp. 1812–1814.

²⁶Page, A. B. and Steinberg, M. L., “High-fidelity simulation testing of control allocation methods,” *AIAA Guidance, Navigation, and Control Conference and Exhibit*, Monterey, CA, Aug. 2002.

²⁷ADMIRE ver. 3.4h, *Aerodata Model in Research Environment (ADMIRE), version 3.4h*, Swedish Defence Research Agency (FOI), 2003, URL: www.foi.se/admire.